JOURNAL OF SOLID STATE CHEMISTRY 113, 257–260 (1994)

The Crystal Structure of Mn_3As_2(III)

Martin F. Hagedorn and Wolfgang Jeitschko[1]

Anorganisch-Chemisches Institut, Universität Münster, Wilhelm-Klemm-Strasse 8, D-48149 Münster, Germany

Received December 14, 1993; accepted February 14, 1994

Single crystals of a third modification of Mn_3As_2 were obtained by chemical transport from 780 to 730°C of prereacted samples in sealed silica tubes in the presence of iodine. This compound is the major reaction product when the elemental components are annealed in the appropriate ratio at 650°C. The structure was determined from single-crystal diffractometer data: $C2/m$, a = 1324.7(3) pm, b = 369.5(1) pm, c = 904.6(4) pm, β = 132.23(3)°, Z = 4, R = 0.024 for 34 variables and 553 structure factors. It is closely related to the structures of V_3As_2 and Ti_5Te_4. The similarities and the differences in the near-neighbor coordinations of the three Mn_3As_2 modifications are discussed. © 1994 Academic Press, Inc.

INTRODUCTION

The phase diagram of the manganese–arsenic system was reassessed by Okamoto (1), based mainly on previous work by Schoen (2) and Yuzuri and Yamada (3). According to these authors, several phases exist in the compositional range between Mn_2As and MnAs. Recently, the structures of two modifications of Mn_3As_2 were reported. Mn_3As_2(I), with the exact composition $Mn_{2.89}As_2$, is a high-temperature phase with a tendency for twinning (4). Upon cooling this phase seems to decompose to intergrown crystals of Mn_3As_2(II) and Mn_5As_4 with very closely related structures (5). The compound Mn_3As_2(III), reported here, is obtained at lower temperatures. At least one more compound exists in this compositional range, for which we determined the composition to be Mn_4As_3 (6). A preliminary account of the present work has appeared previously (7).

SAMPLE PREPARATION

Mn_3As_2(III) was prepared by reaction of the powdered elements manganese (Heraeus, −325 mesh, 99.95%) and arsenic (Ventron, pieces <1.3 cm). The arsenic was ground and purified by fractional sublimation prior to the reactions. Samples with starting compositions between 5:3 and 4:3 were annealed in evacuated silica tubes at 600–650°C for a week. The powder patterns of the dark gray products showed Mn_3As_2(III) as the major phase and often also as the only phase. A well-crystallized sample of this arsenide was obtained by chemical vapor transport of the ground product in the presence of iodine with a charge temperature of 780°C, a growth zone temperature of 730°C, and a reaction time of 10 days.

Energy dispersive X-ray analyses revealed no impurity elements heavier than neon. The crystals are needle-shaped, brittle, gray with a metallic luster, and stable in air. They are slightly attacked by water, the color changing to brown within 1 day.

STRUCTURE DETERMINATION

Crystals of Mn_3As_2(III) were investigated on a Weissenberg camera to find a specimen suitable for the collection of the intensity data. They showed a C-centered monoclinic cell. The cell constants were obtained by a least-squares fit of Guiner powder data (Table 1) using α-quartz (a = 491.30 pm, c = 540.46 pm) as a standard: a = 1324.7(3) pm, b = 369.5(1) pm, c = 904.6(4) pm, β = 132.23(3)°, V = 0.3279 nm^3. A single crystal with the dimensions 0.2 × 0.02 × 0.02 mm^3 was mounted on an automated four-circle diffractometer (Enraf–Nonius CAD4) and intensity data were recorded using graphite-monochromated Mo$K\alpha$ radiation, a scintillation counter, and a pulse-height discriminator. The background was measured on both sides of each $\theta/2\theta$ scan. The intensities of 2839 reflections were recorded within the whole reciprocal space up to 2θ = 70° and an empirical absorption correction was applied using psi-scan data. The ratio of the highest to the lowest transmission was 1.19. Equivalent reflections were averaged (internal residual R_i = 0.026) and weak reflections ($<3\sigma$) were omitted.

The positional parameters of the atoms were determined by Patterson and successive Fourier syntheses. The structure model was then refined by full-matrix least-squares cycles using atomic scattering factors (9) corrected for anomalous dispersion (10). A parameter correcting for secondary isotropic extinction was refined and the weighting scheme included a term based on the counting statistics. Refining the occupancy and the ther-

[1] To whom correspondence should be addressed.

0022-4596/94 $6.00

TABLE 1
Guinier Powder Pattern of Mn_3As_2(III)[a]

h	k	l	Q_o	Q_c	I_o	I_c
0	0	1	222	223	vw	5
2	0	−1	228	229	vw	3
1	1	−1	854	855	m	17
0	0	2	—	892	—	3
4	0	−2	919	918	w	14
2	0	1	1048	1048	m	19
4	0	−3	1213	1214	vw	4
1	1	1	1264	1264	m	20
3	1	−1	1276	1277	m	23
1	1	−2	1315	1319	m	17
3	1	−2	1331	1332	s	57
4	0	0	1666	1663	m	10
3	1	0		1668		27
3	1	−3	1840	1833	vs	92
4	0	−4	—	1956	—	3
6	0	−3	2064	2065	w	9
2	0	2	2125	2126	s	49
1	1	2	2139	2137	m	34
1	1	−3	2229	2229	m	36
5	1	−3	—	2268	—	5
2	0	−4	—	2345	—	3
6	0	−4	2397	2398	m	42
5	1	−1	2531	2531	vs	100
6	0	−1	—	2737	—	4
3	1	−4	2776	2779	m	25
0	2	0	2929	2930	vs	56
6	0	−5	—	3176	—	6
1	1	3	—	3456	—	4
1	1	−4	—	3584	—	8
2	0	3	—	3649	—	9
7	1	−4	—	3663	—	3
8	0	−4	—	3671	—	4
8	0	−3	3749	3748	vw	10

[a] The diagram was recorded with Cu$K\alpha_1$ radiation. All observed reflections and all reflections with calculated intensities $I_c > 2$ are given. The Q values are defined by $Q = 100/d^2$ (nm^{-2}). For the intensity calculations (8), the positional parameters of the refined structure were used.

mal parameters together revealed no deviations from the ideal occupancy values greater than 0.9%. Therefore the ideal occupancies were assumed for the final cycles. A conventional residual of $R = 0.024$ resulted for 553 structures factors and 34 variable parameters. The final difference Fourier synthesis showed the values of ± 0.8 e$^-$/Å^3 as the highest and lowest densities. The final positional parameters and interatomic distances are listed in Tables 2 and 3. The anisotropic thermal parameters and the structure factors are available from the authors.

TABLE 2
Atomic Parameters of Mn_3As_2(III)[a]

Atom	C2/m	x	y	z	B
Mn1	4i	0.30820(9)	0	0.6832(1)	0.88(2)
Mn2	4i	0.38883(8)	0	0.0869(1)	0.83(2)
Mn3	2d	0	½	½	1.23(3)
Mn4	2a	0	0	0	0.78(3)
As1	4i	0.06069(6)	0	0.34317(8)	0.78(1)
As2	4i	0.24682(6)	0	0.17768(8)	0.76(1)

[a] The atomic parameters were standardized by the program STRUCTURE TIDY (11). The last column contains the equivalent isotropic B values (×100, in units of nm^2) of the ellipsoidal thermal parameters.

DISCUSSION

The crystal structure of the third modification of Mn_3As_2 (Fig. 1) shows no great similarity to the structures of the other two modifications (4, 5). Both of these can be described as being composed of building elements, which are derived from the NiAs- and Ni_2In-type structures, where the arsenic and indium atoms form hexagonal close-packed arrays. In the structure of Mn_3As_2(III) distorted close-packed layers of arsenic atoms also can be visualized, however, the close-packed sheets formed by the arsenic atoms are rather frequently disrupted by the manganese clusters around the Mn4 atoms, and therefore we do not consider the Mn_3As_2(III) structure to be as closely related to the NiAs- and Ni_2In-type structures as the other two modifications.

TABLE 3
Interatomic Distances of Mn_3As_2(III)[a]

Mn1	1	As1	258.0	Mn4	2	As2	249.2
	2	As2	260.0		2	As1	263.2
	2	As1	265.4		4	Mn2	278.5
	2	Mn4	288.0		4	Mn1	288.0
	1	Mn2	303.5				
	1	Mn2	303.9				
	2	Mn1	314.8	As1	1	Mn1	358.0
					2	Mn2	262.2
Mn2	1	As2	250.8		1	Mn4	263.2
	2	As2	256.7		2	Mn1	265.4
	2	As1	262.2		2	Mn3	275.8
	2	Mn4	278.5				
	1	Mn3	295.6				
	1	Mn1	303.5	As2	1	Mn4	249.2
	1	Mn1	303.9		1	Mn2	250.8
					2	Mn2	256.7
Mn3	2	As2	257.0		1	Mn3	257.0
	4	As1	275.8		2	Mn1	260.0
	2	Mn2	295.6				

[a] All interatomic distances shorter than 340 pm are listed. Standard deviations are equal or less than 0.1 pm.

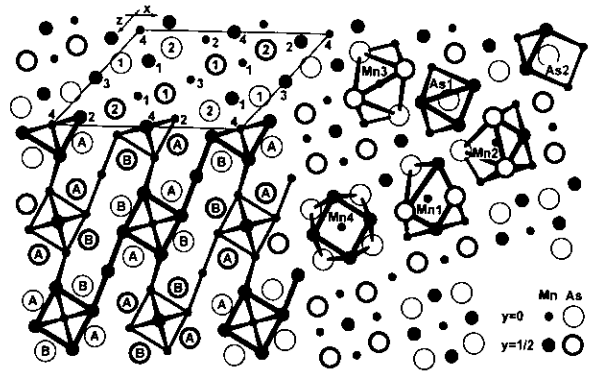

FIG. 1. Crystal structure and coordination polyhedra of Mn_3As_2 (III). The coordination polyhedra correspond to the interatomic distances as listed in Table 3. The numbers in the upper left-hand corner correspond to the atom designations. Distorted hexagonally close-packed arsenic layers are indicated by the letters A and B in the lower left-hand part of the drawing. There also all Mn–Mn bonds shorter than 315 pm shown.

TABLE 4
Comparison of the Average Interatomic Mn–As Distances in the Three Modifications of Mn_3As_2

As coordination of Mn atoms	Mn_3As_2(I)	Mn_3As_2(II)	Mn_3As_2(III)
CN = 6 (octahedral)	Mn1: 272.9 Mn2: 272.5	Mn2: 272.4	Mn3: 269.5
CN = 5 (square pyramidal)	Mn3: 264.0 Mn4: 260.7 Mn6: 265.9	Mn1: 261.8 Mn3: 264.8 Mn5: 263.8	Mn1: 261.8 Mn2: 257.7
CN = 5 (trigonal bipyramidal)	Mn5: 267.3	Mn4: 269.3	—
CN = 4 (tetrahedral)	Mn7: 247.3[a]	Mn6: 249.3	—
CN = 4 (square planar)	—	—	Mn4: 256.2
Mn coordination of As atoms	**Mn_3As_2(I)**	**Mn_3As_2(II)**	**Mn_3As_2(III)**
CN = 8 (bicapped trigonal prism)	As1: 266.3 As2: 269.1	As2: 269.4 As4: 267.8	As1: 266.0
CN = 7 (monocapped trigonal prism)	As3: 259.0[b] As4: 259.9	As1: 259.4 As3: 259.4	As2: 255.8

[a] The Mn7 position of Mn_3As_2(I) is occupied to only 79.1(3)%.
[b] There is a printing error in Table 3 of Ref. (4): the As3 atom has only one Mn2 neighbor.

Nevertheless, many coordination polyhedra are similar in the three modifications. In all modifications the manganese atoms occur in octahedral and square pyramidal arsenic coordination. Trigonal bipyramidal and tetrahedral coordination occur only for the manganese atoms in Mn_3As_2(I) and Mn_3As_2(II), while square planar arsenic coordination of manganese atoms is found only in the structure of Mn_3As_2(III). In addition, each manganese atom forms several weak Mn–Mn bonds in all three modifications. In Mn_3As_2(III) they range between 278.5 and 314.8 pm. In Mn_3As_2(I) this range extends from 278.8 to 329.2 pm, and in Mn_3As_2(II) from 282.4 to 326.7 pm. Only two kinds of coordination occur for the arsenic atom in the three modifications: the bicapped (coordination number (CN) 8) and the monocapped (CN 7) trigonal prism of manganese atoms. There are no bonding As–As interactions in any of the three modifications: the shortest As–As distances are all greater than 340 pm.

The average Mn–As distances of the three modifications are compared in Table 4. As can be expected, these distances reflect the coordination numbers. They range from 247.3 and 249.3 pm for the tetrahedrally coordinated Mn7 and Mn6 atoms of Mn_3As_2(I) and Mn_3As_2(II), respectively, to between 269.5 and 272.9 pm for the octahedrally coordinated manganese atoms of the three modifications. In general, the Mn–As distances are slightly shorter in Mn_3As_2(III) than they are in the other two modifications. This slight difference may be rationalized, at least to some extent, by the differences in the Mn–Mn bonding. For instance, the six different manganese atoms with square pyramidal arsenic coordination of Mn_3As_2(I) and Mn_3As_2(II) have six or seven manganese neighbors (with Mn–Mn distances covering the range 278.8 to 329.2 pm), while the two manganese atoms of Mn_3As_2(III) have only four and five manganese neighbors, respectively. Accordingly, almost all average Mn–As distances of the square pyramidal manganese atoms of modifications I and II are longer than the corresponding distances of Mn_3As_2(III) (cf. Table 4). On the other hand, all manganese atoms of the three modifications with octahedral arsenic coordination have two additional manganese neighbors at comparable distances. Nevertheless, the average Mn–As distances of these manganese atoms are about 3 pm shorter in Mn_3As_2(III) than they are in the other two modifications. This may be caused by "packing effects," which are difficult to analyze in solid-state structures, and it correlates with the fact that Mn_3As_2(III) is that modification, which is stable at the lowest temperature, and generally low-temperature modifications have higher densities. This is indeed the case: the calculated densities are 6.05, 6.12, and 6.37 g/cm^3 for the modifications, I, II, and III, respectively.

The structure of the third modification of Mn_3As_2 is closely related to the structure of V_3As_2 (12). Both may be considered filled-up versions of the Ti_5Te_4-type structure (13), which was found also for the arsenides Mo_5As_4 (14) and Ta_5As_4 (15). To emphasize the relationships of these structures we have transformed the structure of Mn_3As_2(III) to the body-centered monoclinic setting $I2/m$ (Fig. 2), and furthermore we emphasize the metal–metal bonding within the octahedral clusters, which may be

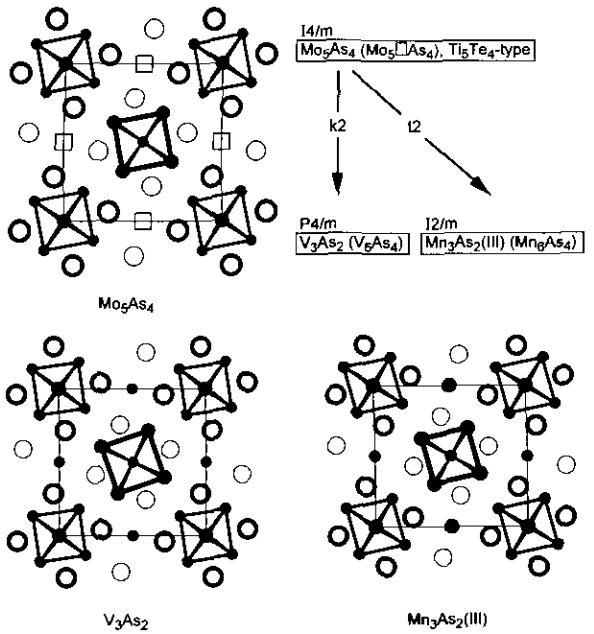

FIG. 2. The crystal structure of Mn_3As_2(III) in the nonstandard setting *I2/m* emphasizing the relationship to the structures of Mo_5As_4 (Ti_5Te_4-type) and V_3As_2. The metal and arsenic atoms are represented by filled and open circles, respectively. Note that the voids (□) in the structure of Mo_5As_4 ($Mo_5□As_4$) are filled by two metal atoms at height 0 of the projection direction in V_3As_2 (V_6As_4) and by one metal atom at height 0 and another metal atom at height 1/2 in Mn_3As_2(III) (Mn_6As_4). The group–subgroup relationships of the three structures are shown in the upper right-hand corner.

regarded as building elements also of related compounds (16). The group–subgroup relationships of the three structure types are shown in Fig. 2 in the manner formalized by Bärnighausen (17). It can be seen, that the voids (□) in the structure of Mo_5As_4 ($Mo_5□As_4$) are filled by metal atoms at $z = 0$ in the structure of V_3As_2 (V_6As_4). This lowers the body-centered tetragonal symmetry *I4/m* of the Ti_5Te_4 type structure of Mo_5As_4 to the primitive tetragonal cell *P4/m* of V_3As_2, where *P4/m* is a *klassengleiche* (*k*) subgroup of *I4/m*. In the structure of Mn_3As_2(III) the additional manganese atoms fill the voids of the Ti_5Te_4-type structure at heights 0 and 1/2 of the projection direction in such a way that the body centering is maintained. Thus, in going from the space group *I4/m* (Ti_5Te_4-type) to the space group *I2/m* of Mn_3As_2(III), the translational symmetry is maintained and only rotational symmetry is lost. The space group *I2/m* of Mn_3As_2(III) is a *translationengleiche* (*t*) subgroup of *I4/m* (18, 19).

ACKNOWLEDGMENTS

We thank Dipl.-Ing. U. Rodewald and Dr. M. H. Möller for collecting the single-crystal diffractometer data and Mr. K. Wanger for the work on the scanning electron microscope. We also acknowledge Dr. G. Höfer (Heraeus Quarzschmelze) for the generous gift of silica tubes. This work was supported by the Deutsche Forschungsgemeinschaft and the Fonds der Chemischen Industrie.

REFERENCES

1. H. Okamoto, *Bull. Alloy Phase Diagr.* **10,** 549 and 607 (1989).
2. P. Schoen, *Metallurgie* **8,** 737 (1911).
3. M. Yuzuri and M. Yamada, *J. Phys. Soc. Jpn.* **15,** 1845 (1960).
4. L. H. Dietrich, W. Jeitschko, and M. H. Möller, *Z. Kristallogr.* **190,** 259 (1990).
5. M. H. Möller and W. Jeitschko. *Z. Kristallogr.* **204,** 77 (1993).
6. M. F. Hagedorn and W. Jeitschko, *Z. Kristallogr.* Suppl. **5,** 93 (1992).
7. M. F. Hagedorn and W. Jeitschko, *Z. Kristallogr.* Suppl. **7,** 67 (1993).
8. K. Yvon, W. Jeitschko, and E. Parthé, *J. Appl. Crystallogr.* **10,** 73 (1977).
9. D. T. Cromer and J. B. Mann, *Acta Crystallogr. Sect. A* **24,** 321 (1968).
10. D. T. Cromer and D. Liberman, *J. Chem. Phys.* **53,** 1891 (1970).
11. L. M. Gelato and E. Parthé, *J. Appl. Crystallogr.* **20,** 139 (1987).
12. R. Berger, *Acta Chem. Scand. Ser. A* **31,** 287 (1977).
13. F. Gronvold, A. Kjekshus, and F. Raaum, *Acta Crystallogr.* **14,** 930 (1961).
14. P. Jensen and A. Kjekshus, *Acta Chem. Scand.* **20,** 1309 (1966).
15. S. Rundqvist, B. Carlsson, and C.-O. Pontchour, *Acta Chem. Scand.* **23,** 2188 (1969).
16. A. Simon, *Angew. Chem.* **93,** 23 (1981).
17. H. Bärnighausen, *Commun. Math. Chem.* **9,** 139 (1980).
18. H. Wondratschek and W. Jeitschko, *Acta Crystallogr. Sect. A* **32,** 664 (1976).
19. T. Hahn (Ed.), "International Tables for Crystallography," Vol. A. Reidel, Dordrecht, 1983.